ACS APPLIED MATERIALS & INTERFACES

Research Article

www.acsami.org

Nucleobase-Functionalized Conjugated Polymer for Detection of Copper(II)

Chengfen Xing,*[,†] Hongbo Yuan,[†] Sichuan Xu,[‡] Hailong An,[†] Ruimin Niu,[†] and Yong Zhan*[,†]

[†]Institute of Biophysics, Hebei University of Technology, Tianjin 300401, P. R. China

[‡]College of Chemical Science and Technology, Yunnan University, Kunming 650091, P. R. China

Supporting Information

ABSTRACT: In recent years, supramolecular organization of thiophene derivatives, oligo- and polythiophene, have been developed with various designs to achieve complex functions. Here, we describe the synthesis and characterization of a conjugated polymer with thymidine side chain bases and polythiophene backbones (PTT) instead of phosphate bonds in DNA, and the PTT exhibits exceptional fluorescence quenching efficiency upon binding of Cu^{2+} ions in aqueous medium, which is suggested to be electron transfer from the π^* orbit at the excited state of PTT to the 3d orbit of Cu^{2+} ions and subsequent Cu^{2+}-mediated interpolymer π-stacking aggregation. Furthermore, Cu^{2+} ions can be selectively and easily monitored by the fluorescence quenching of PTT, which can be used for detection of Cu^{2+} ions with good selectivity and high sensitivity in aqueous medium. Both experimental and theoretical methods have been devoted to demonstrate the strong affinity and steric interaction of PTT toward Cu^{2+}. These findings will illustrate new directions for the design of nucleobase-functionalized materials with transition metals responsive activity.

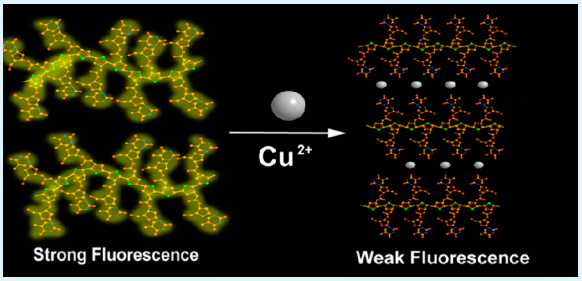

KEYWORDS: *conjugated polythiophene, Cu^{2+}, sensor, thymidine, fluorescence quenching*

INTRODUCTION

Water-soluble conjugated polymers (CPs) are known by delocalized electronic structure and exhibit unique flexibility, thermal stability, and optoelectrical properties. The CPs have large absorption coefficients in comparison to small molecules by collective action of plenty of absorbing units. Extremely high efficiencies of fluorescence quenching or energy transfer take place when the excitation energy along the backbone transfers to the energy or electron acceptor, resulting in the optical signal amplification for chemical or biological sensors.[1−3] They have been extensively studied as active materials for device fabrications including rechargeable batteries, electrochromic devices, solar cells, and chemical/biological sensors.[4−9] The fabrication of metal-containing materials based on CPs is potential for the development of future molecular electronics.[10,11] A promising approach to obtain functional metal-containing materials is to use selective and sensitive donor−acceptor interactions to modulate the elctron transport properties of the conjugated chains of CPs.[12,13] Transition metals are utilized for functionalization of CPs in various modification systems by using as good carriers of many functions.[14,15]

In this work, we combine the advantages of CPs and transition metals to obtain Cu^{2+}-containing complex with selective and sensitive Cu^{2+} responsive activity in aqueous media. We synthesize and characterize a nonionic water-soluble polythiophene (PTT) containing thymidine side chain bases and polythiophene backbones instead of phosphate bonds in DNA. The PTT combines the unique molecular recognition capacity of nucleobases and the photophysical features of polythiophenes.[16−18] Upon adding Cu^{2+} ions, the large interaction energy of Cu^{2+} with PTT is the favorite to the formation of PTT−Cu^{2+} complexes according to theoretical calculations, so that the unique fluorescence response of PTT is observed. In this context, PTT can be used to assay Cu^{2+} ions selectively and sensitively and can be easily monitored by the fluorescence quenching of PTT (Scheme 1). Although several polythiophene-nucleobase conjugates have been developed so far,[19−22] less was exploited for the Cu^{2+}-containing complex for specific recognition in aqueous media.

EXPERIMENTAL SECTION

Materials and Instruments. All chemicals were purchased from Aldrich Chemical Co. or Alfa-Aesar and used without further purification. Solvent pyridine was distilled from potassium hydroxide, and chloroform was distilled from calcium hydride. The ^{1}H NMR and ^{13}C NMR spectra were measured on a Bruker Avance 400 MHz spectrometer. Elemental analyses were performed with a Flash EA1112 instrument. The gel permeation chromatography (GPC) measurements were carried out on a Waters-410 system against polystyrene standards with DMF as an eluent. The fluorescence spectra were measured on a Hitachi F-4500 fluorometer using a xenon-lamp as the excitation source. The excitation wavelength is 405 nm. UV−vis

Received: April 2, 2014
Accepted: June 3, 2014
Published: June 3, 2014

   dx.doi.org/10.1021/am502978w | ACS Appl. Mater. Interfaces 2014, 6, 9601−9607

Scheme 1. Schematic Cu^{2+} Ions Detection in Aqueous Medium

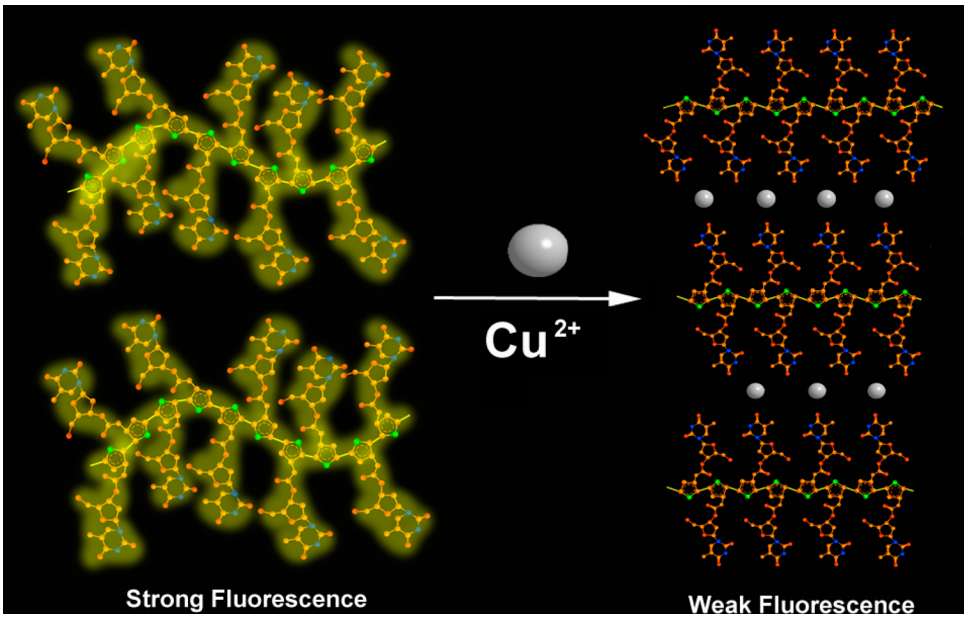

absorption spectra were carried out on a JASCO V-550 spectrometer. Field emission scanning electron microscopy (SEM) images were taken from a Hitachi S-4800 FESEM microscope at an accelerating voltage of 10 kV. Atomic force micrographs (AFM) were obtained by a Nanoscope IIIa atomic force microscope using tapping mode. Dynamic light scattering (DLS) measurements were recorded on a Malvern Nano-ZS ZEN 3600 instrument.

Synthesis of 5′-*O*-(4,4′-Dimethoxytrytil) Thymidine (2). Thymidine **1** (2.42 g, 10 mmol) was added into 30 mL of dry pyridine, and the suspension was treated with 4′,4′-dimethoxytrityl chloride (4.07 g, 12 mmol) at room temperature for 3 h, after which the reaction was quenched with 2 mL of methanol at 0 °C. The solvent was concentrated under vacuum, and the crude product was purified by silica gel chromatography with $MeOH/CH_2Cl_2$ (1/10) as the eluent to give a solid (4.4 g, 81%). ^1H NMR (300 MHz, $CDCl_3$): δ (ppm) 1.47 (s, 3H), 2.36 (m, 1H), 2.43 (m, 2H), 3.35 (d, 1H, J = 2.4), 3.38 (d, 1H, J = 2.4), 3.79 (s, 6H), 4.05 (d, 1H, J = 2.4), 4.58 (s, 1H), 6.42 (t, 1H, J = 13.5), 6.84 (d, 4H, J = 8.6), 7.24 (m, 7H), 7.39 (d, 2H, J = 7.5), 7.59 (s, 1H), 8.56 (br, 1H, NH). MS-EI: 544 (M^+).

Synthesis of 3′-*O*-[2-(3-Thiphene)-acetyl]-5′-*O*-(4,4′-dimethoxytrytil) Thymidine (3). To a mixture of compound **2** (4.34 g, 8 mmol) and 2-(3-thienyl)-acetic acid (1.136 g, 8 mmol) in 30 mL of dry $CHCl_3$ was added EDCI (1.92 g, 10 mmol). After the reaction mixture was stirred for 30 min at room temperature, DMAP (0.98 g, 8 mmol) was added and the mixture was further stirred for 12 h. The solvent was concentrated under vacuum, and the crude product was puried by silica gel chromatography with $MeOH/CH_2Cl_2$ (1/50) as eluent to give a solid (4.6 g, 86%). ^1H NMR (400 MHz, $CDCl_3$): δ (ppm) 1.42 (s, 3H), 2.38 (m, 1H), 2.43 (m, 2H), 3.47 (m, 2H), 3.60 (s, 2H), 3.68 (s, 1H), 3.78 (s, 6H), 3.92(s, 1H), 4.10 (s, 1H), 4.58 (s, 1H), 5.48 (s, 1H), 6.43 (t, 1H, J = 13.5), 6.82 (d, 4H, J = 8.7), 7.15 (m, 1H), 7.24 (m, 2H), 7.29 (m, 7H), 7.37 (d, 2H, J = 7.4), 7.60 (s, 1H), 8.43 (br, 1H, NH). ^{13}C NMR: (100 MHz, $CDCl_3$, ppm) δ: 11.56, 35.63, 37.84, 55.21, 63.64, 75.82, 83.99, 84.29, 87.18, 111.65, 113.13, 113.29, 123.11, 126.05, 127.73, 128.0, 128.21, 129.01, 130.03, 132.71, 135.10, 135.18, 135.31, 139.45, 144.15, 150.38, 158.59, 163.49, 170.55. MALDI-TOF: 691.1 [M + Na]. Anal. Calcd for $C_{37}H_{36}O_8N_2S$: C 66.45, H 5.43, N 4.19. Found: C 67.07, H 5.38, N 4.16.

Synthesis of 3′-*O*-[2-(3-Thiphene)-acetyl] Thymidine (4). To a solution of compound **3** (4.01 g, 6 mmol) in 47.5 mL of dry $CHCl_3$ was added 2.5 mL of CF_3COOH, and the reaction mixture was stirred for 30 min at room temperature. The solvent was concentrated under vacuum, and the crude product was purified by silica gel chromatography with $MeOH/CH_2Cl_2$ (1/10) as eluent to give a solid (1.8 g, 82%). ^1H NMR (400 MHz, DMSO-d_6): δ (ppm) 1.94 (s, 3H), 2.28 (m, 2H), 3.40 (br, 1H, OH), 3.61 (s, 2H), 3.75 (s, 2H), 3.97 (s, 1H), 5.25 (d, 2H, J = 5.7), 6.19 (m, 1H), 7.05 (d, 1H, J = 4.9), 7.35 (d, 1H, J = 2.6), 7.49 (m, 1H), 7.37 (s, 1H), 11.33 (s, 1H, NH). ^{13}C NMR: (100 MHz, DMSO-d_6) δ: (ppm) 12.69, 35.30, 36.87, 61.74, 75.60, 84.09, 84.95, 110.15, 123.65, 126.43, 129.20, 134.14, 136.22, 150.88, 164.07, 170.81. MS-EI: 366 (M). Anal. Calcd for $C_{16}H_{18}O_6N_2S$: C 52.45, H 4.95, N 7.65. Found: C 52.87, H 4.86, N 7.58.

Synthesis of PTT. Under nitrogen, anhydrous $FeCl_3$ (0.486 g, 3 mmol) in dry $CHCl_3$ (5 mL) of was stirred for 30 min. To this suspension was added a solution of compound **4** (0.183 g, 0.5 mmol) in 5 mL of $CHCl_3$. The reaction was quenched by adding methanol after stirring for 48 h at room temperature. The filtrate after filtration was washed with CH_3OH (30 mL × 3), and the crude product was dissolved in 5 mL of DMSO followed by adding 0.5 mL of hydrazine. The mixture was stirred for 4 h at room temperature, and the solvent was concentrated under vacuum to yield a yellow amorphous solid (0.082 g, 45%). ^1H NMR (400 MHz, DMSO-d_6): δ (ppm) 1.76 (br, 3H), 1.91 (br, 2H), 3.62−3.71 (br, 3H), 3.99 (br, 2H), 4.88−5.25 (br, 2H), 6.19 (br, 1H), 7.17 (br, 1H), 7.72(br, 1H), 11.28 (br, 1H, NH). ^{13}C NMR: (100 MHz, DMSO-d_6) δ: (ppm) 12.67, 36.92, 49.01, 61.73, 76.07, 84.16, 84.96, 110.14, 132.53, 136.19, 150.86, 164.06, 170.10. GPC: M_n = 25 700, M_w = 62 700, PDI = 2.44.

Fluorescence Quenching Experiment of PTT by Cu^{2+} Ions. Cu^{2+} ions ([Cu^{2+}] = 0−5 μM) was added successively to a solution of PTT ([PTT] = 7.3 × 10^{-3} mg/mL) in Tris-HCl buffer (5 mM, pH = 7.4) at room temperature. The samples were incubated at room temperature for 1 min, and then the fluorescence spectra were measured at an excitation wavelength of 405 nm.

Simulation and Computations. The geometry of monomer **4** was fully optimized at the B3LYP/6-31G(d,p) level in the Gaussian 03 program and characterized as a minimum with no imaginary frequency. The PTT structure for molecular dynamics (MD) simulation was built individually by using the optimized geometry of monomer **4**. The MD simulation of PTT was carried out with the Gromacs 3.3.3 software package. Subsequent analysis scripts were all packaged with the Gromacs. The software package VMD was used for the visualization of simulation trajectories.[23] PTT molecular parameters were defined as follows. The gmx-united atom types were used in the MD simulation of PTT, where CH, CH_2, and CH_3 groups are represented as a single atom. Mulliken atomic charges with hydrogen's ones summed into heavy atoms, obtained by calculation

Scheme 2. Schematic Preparation of PTT

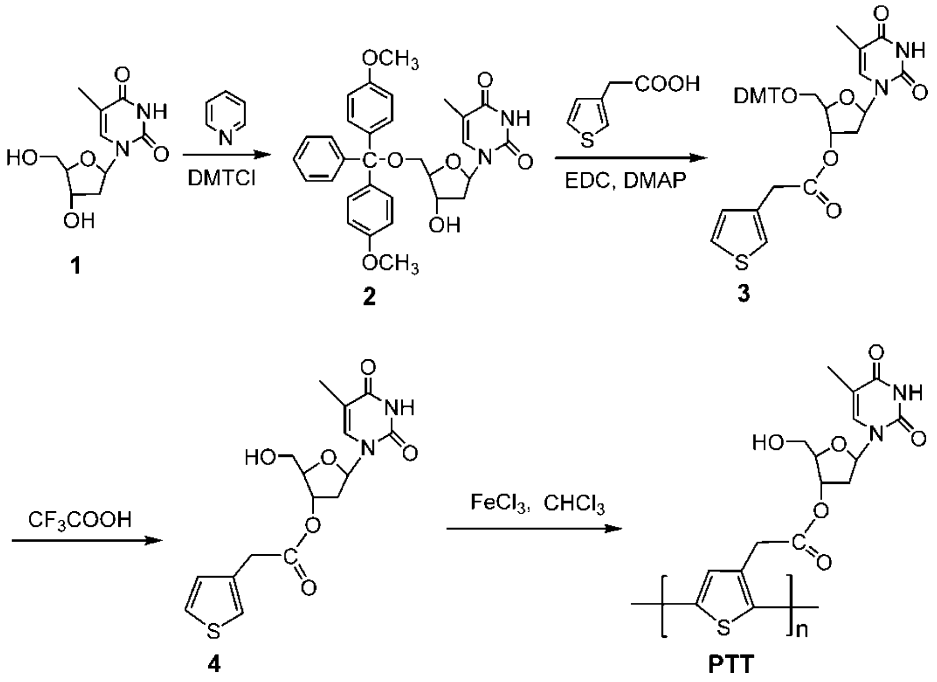

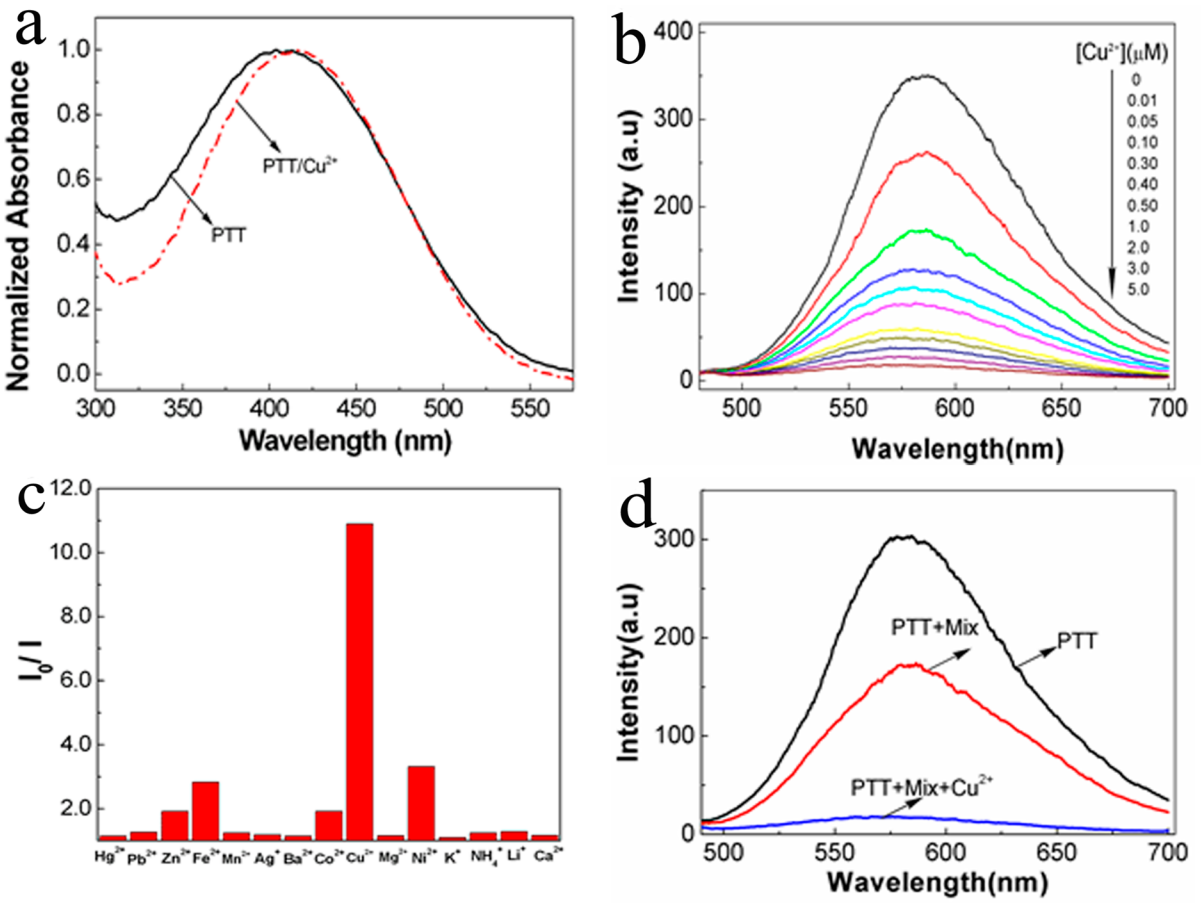

Figure 1. (a) UV−vis spectra of PTT and PTT/Cu^{2+} in Tris-HCl buffer (5 mM, pH = 7.4). [PTT] = 7.3×10^{-3} mg/mL, [Cu^{2+}] = 5×10^{-6} M. (b) Fluorescence spectra of PTT in Tris-HCl buffer (5 mM, pH = 7.4) with successive addition of Cu^{2+}. [PTT] = 7.3×10^{-3} mg/mL, [Cu^{2+}] = 0−5 μM. (c) Fluorescence quenching efficiencies of PTT with metal ions (each 5.0×10^{-6} M) in Tris-HCl buffer (5 mM, pH = 7.4). [PTT] = 7.3×10^{-3} mg/mL. (d) Fluorescence spectra of solutions with PTT, metal ions mixture (mix, Fe^{2+}, Hg^{2+}, Co^{2+}, and Zn^{2+}, each 5×10^{-6} M) and Cu^{2+} in Tris-HCl buffer. The excitation wavelength is 405 nm.

dx.doi.org/10.1021/am502978w | ACS Appl. Mater. Interfaces 2014, 6, 9601−9607

using B3LYP/6-31G (d,p), were adopted for PTT molecule. Bond and angle parameters of PTT molecule were defined according to bonds and angles in the optimized geometry of monomer **4**. Improper dihedral parameters were also defined to better strain molecules into the proper configurations during simulation. Gmx force fields[24] were used for the MD simulation of PTT. During simulation, the PTT structure was immersed in an octahedron box of SPC water.[25] The buffer is 2.0 nm between the PTT atoms and the edge of the box. The sum of chemical bonds, bond twists, bond angles, hydrogen bonds, van der Waals, and electrostatic is defined to contribute to the potential energy of the system. When the MD optimization of PTT was set at a termination standard of 100 kJ/mol, the steepest descent energy minimization was used to remove bad van der Waals contacts between atoms. Next, the MD solute position-restrained by the LINCS algorithm,[26] while restraining the atom positions of PTT and letting the solvent move in the simulation, was performed to soak for 200 ps. Then, the simulation of 10 ns MD followed. The calculations used a 2 fs step with coordinates were written to the output file once every 2000 steps (4 ps). The pair list of neighbors was updated every 10 steps for calculating nonbonding interactions. Periodic boundary conditions were performed on the simulation box, along with a cutoff distance of 1.0 nm for electrostatic interactions and 1.0 nm for Lennard-Jones nonbonding interactions. PME procedure with default parameters was applied to describe the long-range electrostatic effect. The Berendsen thermostat was used for temperature coupling with a time constant of 0.1 ps. The Berendsen exponential relaxation pressures coupling with the time constant 0.5 ps were applied.[27] VMD was used to combine and view the trajectory data and frames written by simulation. The new saved structure of PTT was used for docking assignment. The whole PTT structure is considered as a field for small molecules to dock. According to the protocol of docking program,[28] small molecules were docked to PTT. The ranked orientation obtained by the docking experiment was normally specified as the minimum conformation of the small molecule combined with PTT together using the Chimera program.[29]

RESULTS AND DISCUSSION

The procedures of PTT preparation are shown in Scheme 2. Reaction of thymidine (**1**) and 4,4-dimethoxytrityl chloride in anhydrous pyridine at room temperature provides 5′-*O*-(4,4-dimethoxytrytil) thymidine (**2**) in 81% yield. The 3′-*O*-[2-(3-thiphene)-acetyl]-5′-*O*-(4,4′-dimethoxytrytil) thymidine (**3**) was synthesized by coupling compound **2** with 2-(3-thienyl)-acetic acid in 86% yield.[30] Treatment of compound **3** with 5% CF_3COOH in $CHCl_3$ to deprotect the DMT groups affords 3′-*O*-[2-(3-thiphene)-acetyl] thymidine (**4**) in 82% yield. PTT was obtained by oxidative polymerization of monomer **4** in $CHCl_3$ with $FeCl_3$ as the oxidation reagent.[31] PTT is can dissolve in polar solvents such as DMF, DMSO, and water readily. Its structure was characterized by ^1H NMR and ^{13}C NMR spectroscopy (see Figure S1 in the Supporting Information). The gel permeation chromatography (GPC) with polystyrene as the standard and DMF as the eluent indicated that the number-average molecular weight (M_n) of PTT is 25 700 and the polydispersity index (PDI) is 2.44.

The absorbance and fluorescence properties of PTT were studied in water. The absorption peak of PTT was 410 nm, corresponding to the $\pi-\pi^*$ transition of conjugated units. The PTT exhibits yellow fluorescence with irradiation and the emission spectra shows the emission maximum at 575 nm, which is the characteristic of polythiophenes.[22] The quantum yield of PTT in water was 5% with quinine sulfate in H_2SO_4 (0.1 M) as the standard.

The selective detection of Cu^{2+} ions can be easily monitored by the fluorescence quenching of PTT. Figure 1a shows the absorption spectra of PTT in the absence and presence of Cu^{2+} ions in Tris-HCl buffer, and we can see the absorption maximum of PTT is red-shifted by 13 nm upon adding Cu^{2+} ions. Figure 1b shows the emission spectra of PTT in Tris-HCl buffer with a constant concentration upon adding Cu^{2+} ions ($[Cu^{2+}] = 0-5 \times 10^{-6}$ M) successively with an excitation wavelength of 405 nm. It exhibits a significant quenching with adding the Cu^{2+} ions and about 95% decrease of emission intensity at 580 nm. The detection limit of Cu^{2+} ions is 10 nM. These results demonstrated that the PTT can be used for detection of Cu^{2+} ions with good selectivity and high sensitivity in aqueous medium. The fluorescence quenching of the PTT along with the red shift (Figure 1a) and the 30% decrease of absorbance (Figure S2 in the Supporting Information) with Cu^{2+} ions indicates the strong interactions of PTT and Cu^{2+} ions, resulting in interpolymer π-stacking aggregation.

To examine the selective recognition of PTT, the fluorescence responses of PTT to other metal ions such as Li^+, NH_4^+, K^+, Ag^+, Ca^{2+}, Mg^{2+}, Ba^{2+}, Fe^{2+}, Ni^{2+}, Co^{2+}, Pb^{2+}, Hg^{2+}, Mn^{2+}, and Zn^{2+} ions were also examined (Figure 1c). The addition of Li^+, NH_4^+, K^+, Ca^{2+}, Mg^{2+}, Ba^{2+}, Ag^+, Mn^{2+}, Pb^{2+}, or Hg^{2+} ions cannot change the fluorescence of PTT. Although adding Fe^{2+}, Ni^{2+}, Co^{2+},or Zn^{2+} ions could induce slight fluorescence quenching, the fluorescence decreases are 3−4 times less than that for Cu^{2+} ions, indicating PTT possesses specific recognition ability for Cu^{2+} ions. It is important to study the interference from other mixed metal ions for the assay of Cu^{2+} ions. The fluorescence emission spectra of the PTT to Cu^{2+} ions was measured with other metal ions (Figure 1d). The PTT was quenched approximately 40% by adding mixed metal ions (Fe^{2+}, Hg^{2+}, Co^{2+}, and Zn^{2+}) to the aqueous solution of PTT. Upon adding Cu^{2+} ions to the mixture solution, there was a significant fluorescence intensity decrease and the quenching efficiency reached 95% approximately. These results indicate that the PTT can recognize Cu^{2+} ions in water with minor interference.

To validate the formation of the nanocomposites of PTT/Cu^{2+} in aqueous solution, we conducted dynamic light scattering (DLS) measurements which were performed in Tris-HCl buffer. The average hydrodynamic radius of PTT/Cu^{2+} is 151 nm (Figure 2), which is 3.5 times larger than that of PTT itself, indicating the formation of larger assembly upon addition of Cu^{2+} in aqueous solution. However, the average hydrodynamic radius become slightly smaller by the addition of Hg^{2+}, demonstrating the PTT can form aggregation induced

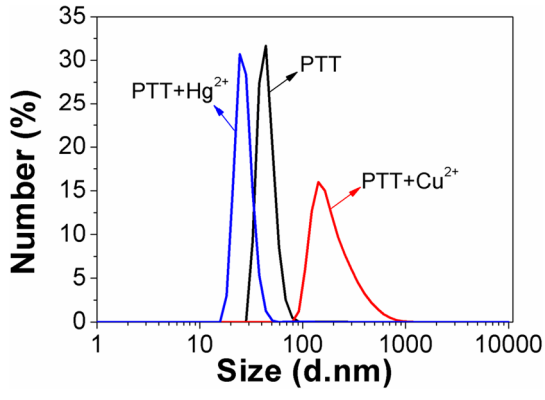

Figure 2. Dynamic light scattering traces of PTT, PTT + Hg^{2+}, and PTT + Cu^{2+} in Tris-HCl buffer. [PTT] = 7.3×10^{-3} mg/mL, $[Hg^{2+}] = [Cu^{2+}] = 5 \times 10^{-6}$ M.

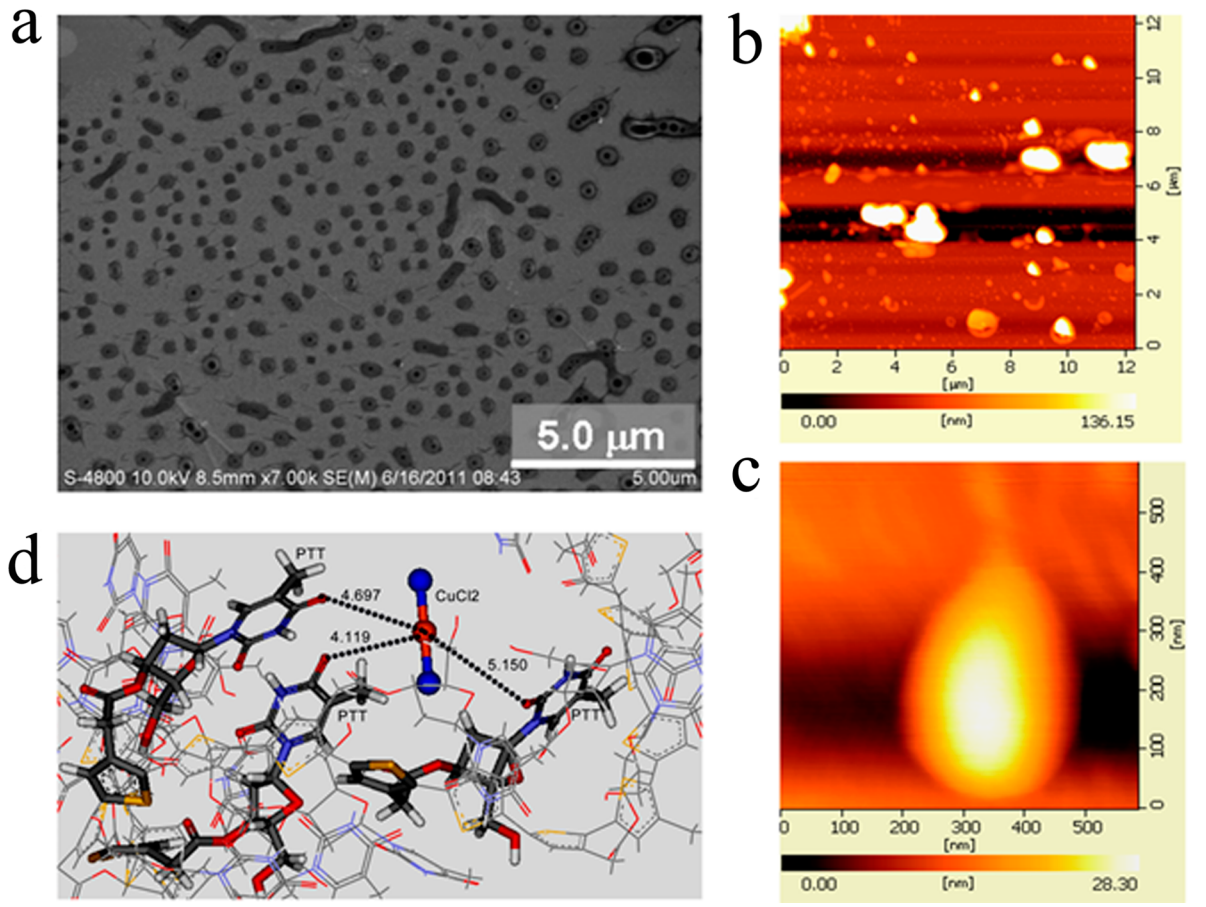

Figure 3. (a) SEM images and (b) lower magnification and (c) higher magnification of AFM images of PTT/Cu^{2+} complex. [PTT] = 3.7×10^{-2} mg/mL, [Cu^{2+}] = 2×10^{-6} M. (d) The interaction of Cu^{2+} with PTT obtained by the docking experiment. The optimized geometries are calculated with B3LYP/3-31G. The PTT with six repeated units was used for the simulation.

specifically by Cu^{2+} ions. These results give more evidence of the strong affinity of PTT toward Cu^{2+} in aqueous solution.

The morphology of the PTT/Cu^{2+} complex was examined by SEM. As shown in Figure 3a and Figure 3S in the Supporting Information, the PTT/Cu^{2+} forms homogeneous nanoparticles with the size of 300−500 nm. AFM visualizes the shape and dimensions of PTT/Cu^{2+} nanoparticles. After incubation of PTT with Cu^{2+} in aqueous solution, 5.0 μL of solution was dropped onto substrate and the substrate was dried, resulting in a significant increase in the observed height of localized regions on the PTT/Cu^{2+} complexes (Figure 3b). Figure 3c shows a magnified view of one PTT/Cu^{2+} nanoparticle, and the raised height of central area suggests the nanoparticle has three-dimensional structure. In order to obtain insight into the driving force of the formation of PTT/Cu^{2+} complex, the interactions of PTT with Cu^{2+} were examined by theoretical calculations.[32,33] The simulated PTT structure is not linear but contains several curves. These curves may be regarded as the active sites for small molecules to interact with PTT. As shown in Figure 3d, one $CuCl_2$ molecule contacts with three active parts congregated near a curve in the PTT structure. The $CuCl_2$ molecule faces the thymidine groups and is located at a center among three thymidine groups according to the distances labeled in Figure 3d. The interaction energies for $CuCl_2$ and other metal compounds with PTT are obtained by molecular docking and listed in Table S1 in the Supporting Information, which can be used to qualitatively explain the fluorescence response of PTT in Figure 1. The biggest value of −47.0 kJ/mol comes from $CuCl_2$ with PTT, corresponding to the largest fluorescence response of PTT with $CuCl_2$. The similar interaction energies of $ZnCl_2$ and $CoCl_2$ with PTT are consistent with the similar fluorescence responses of PTT. The smaller interaction energies of $MgCl_2$ and AgCl with PTT result in the very small fluorescence responses of PTT. Considering the fluorescence responses of PTT, the interaction energies of metal ions with PTT, the mechanism for metal ions to possess the fluorescence response of PTT is suggested to be electron transfer from the π^* orbit at the excited state of PTT to the 3d orbit of the metal. The $FeCl_2$, $CoCl_2$, $NiCl_2$, $CuCl_2$, and $ZnCl_2$ compounds that have empty 3d orbitals for electron transfer possess the fluorescence response of PTT in Figure 1. The biggest interaction energy of $CuCl_2$ with PTT is the favorite to electron transfer, so that the largest fluorescence response of PTT is observed. Because Ag^+ and Mg^{2+} have no empty 3d orbitals for electron transfer, the very small fluorescence response of PTT is expected in the experiment.

CONCLUSIONS

In conclusion, we describe the synthesis and characterization of PTT containing thymidine side chain bases and polythiophene backbones. The PTT exhibits exceptional fluorescence quenching efficiency upon binding of Cu^{2+} ions in aqueous medium, which is suggested to be electron transfer from the π^* orbit at the excited state of PTT to the 3d orbital of Cu^{2+} ions

and subsequent Cu^{2+}-mediated interpolymer π-stacking aggregation. The PTT can be used as a fluorescent sensor to probe Cu^{2+} ions selectively and sensitively in aqueous medium with minor interference. Both experimental and theoretical methods have been devoted to demonstrate the strong affinity and steric interaction of PTT toward Cu^{2+}. These findings will illustrate new directions for the design of nucleobase-functionalized nanomaterials with transition metals responsive activity.

■ ASSOCIATED CONTENT

Supporting Information

^{1}H NMR and ^{13}C NMR spectra of PTT, UV−vis spectra of PTT and PTT/Cu^{2+}, SEM images of PTT−Cu^{2+} complex and the interaction energies for compounds with PTT obtained by molecular docking, and supplementary figures. This material is available free of charge via the Internet at http://pubs.acs.org.

■ AUTHOR INFORMATION

Corresponding Authors

*E-mail: xingc@hebut.edu.cn.

*E-mail: zhan_yong2014@163.com.

Author Contributions

C. X. and Y.Z. designed the experiments, analyzed the data, and organized the manuscript. H.Y. and R.N. performed the experimental part. S.X. performed the theoretical part. H.A. analyzed the data.

Notes

The authors declare no competing financial interest.

■ ACKNOWLEDGMENTS

This work was supported by the Scientific Innovation Grant for Excellent Young Scientists of Hebei University of Technology (Grant No. 2013003). The authors acknowledge Prof. Libing Liu (Institute of Chemistry, Chinese Academy of Sciences) for valuable suggestion on the work.

■ REFERENCES

(1) Thomas, S. W.; Joly, G. D.; Swager, T. M. Chemical Sensors Based on Amplifying Fluorescent Conjugated Polymers. *Chem. Rev.* **2007**, *107*, 1339−1386.

(2) Zhu, C.; Liu, L.; Yang, Q.; Lv, F.; Wang, S. Water-Soluble Conjugated Polymers for Imaging, Diagnosis, and Therapy. *Chem. Rev.* **2012**, *112*, 4687−4735.

(3) Feng, L.; Zhu, C.; Yuan, H.; Liu, L.; Lv, F.; Wang, S. Conjugated Polymer Nanoparticles: Preparation, Properties, Functionalization and Biological Applications. *Chem. Soc. Rev.* **2013**, *42*, 6620−6633.

(4) Beaujuge, P. M.; Reynolds, J. R. Color Control in Pi-Conjugated Organic Polymers for Use in Electrochromic Devices. *Chem. Rev.* **2010**, *110*, 268−320.

(5) Grimsdale, A. C.; Chan, K. L.; Martin, R. E.; Jokisz, P. G.; Holmes, A. B. Synthesis of Light-Emitting Conjugated Polymers for Applications in Electroluminescent Devices. *Chem. Rev.* **2009**, *109*, 897−1091.

(6) Peet, J.; Heeger, A. J.; Bazan, G. C. Plastic″ Solar Cells: Self-Assembly of Bulk Heterojunction Nanomaterials by Spontaneous Phase Separation. *Acc. Chem. Res.* **2009**, *42*, 1700−1708.

(7) Heeger, A. J.; Sariciftci, N. S.; Namdas, E. B. *Semiconducting and Metallic Polymers*, 1st ed.; Oxford University Press: New York, 2010.

(8) Thomas, S. W., III; Joly, G. D.; Swager, T. M. Chemical Sensors Based on Amplifying Fluorescent Conjugated Polymers. *Chem. Rev.* **2007**, *107*, 1339−1386.

(9) Duan, X. R.; Liu, L. B.; Feng, F. D.; Wang, S. Cationic Conjugated Polymers for Optical Detection of DNA Methylation, Lesions, and Single Nucleotide Polymorphisms. *Acc. Chem. Res.* **2010**, *43*, 260−270.

(10) Fan, L.-J.; Jones, W. E. A Highly Selective and Sensitive Inorganic/Organic Hybrid Polymer Fluorescence "Turn-on" Chemosensory System for Iron Cations. *J. Am. Chem. Soc.* **2006**, *128*, 6784−6785.

(11) Mangeney, C.; Lacroix, J. C.; Chane-Ching, K. I.; Jouini, M.; Villain, F.; Ammar, S.; Jouini, N.; Lacaze, P. C. Conducting-Polymer Electrochemical Switching as an Easy Means for Control of the Molecular Properties of Grafted Transition Metal Complexes. *Chemistry* **2001**, *7*, 5029−5040.

(12) Xing, C.; Yu, M.; Wang, S.; Shi, Z.; Li, Y.; Zhu, D. Fluorescence Turn-On Detection of Nitric Oxide in Aqueous Solution Using Cationic Conjugated Polyelectrolytes. *Macromol. Rapid Commun.* **2007**, *28*, 241−245.

(13) Xing, C.; Shi, Z.; Yu, M.; Wang, S. Cationic Conjugated Polyelectrolyte-Based Fluorometric Detection of Copper(II) Ions in Aqueous Solution. *Polymer* **2008**, *49*, 2698−2703.

(14) Zinchenko, A. A.; Baigl, D.; Chen, N.; Pyshkina, O.; Endo, K.; Sergeyev, V. G.; Yoshikawa, K. Conformational Behavior of Giant DNA through Binding with Ag+ and Metallization. *Biomacromolecules* **2008**, *9*, 1981−1987.

(15) Li, G.; Liu, H.; Chen, X.; Zhang, L.; Bu, Y. Multi-Copper-Mediated DNA Base Pairs Acting as Suitable Building Blocks for the DNA-Based Nanowires. *J. Phys. Chem. C* **2011**, *115*, 2855−2864.

(16) Mishra, A.; Ma, C.-Q.; Bäuerle, P. Functional Oligothiophenes: Molecular Design for Multidimensional Nanoarchitectures and Their Applications. *Chem. Rev.* **2009**, *109*, 1141−1276.

(17) Osaka, I.; McCullough, R. D. Advances in Molecular Design and Synthesis of Regioregular Polythiophenes. *Acc. Chem. Res.* **2008**, *41*, 1202−1214.

(18) Ho, H. A.; Najari, A.; Leclerc, M. Optical Detection of DNA and Proteins with Cationic Polythiophenes. *Acc. Chem. Res.* **2008**, *41*, 168−178.

(19) Bäuerle, P.; Emge, A. Specific Recognition of Nucleobase-Functionalized Polythiophenes. *Adv. Mater.* **1998**, *3*, 324−330.

(20) Bazaco, R. B.; Gómez, R.; Seoane, C.; Bäuerle, P.; Segura, J. L. Specific Recognition of a Nucleobase-Functionalized Poly(3,4-Ethylenedioxithiophene) (PEDOT) in Aqueous Media. *Tetrahedron Lett.* **2009**, *50*, 4154−4157.

(21) Navacchia, M. L.; Favaretto, L.; Treossi, E.; Palermo, V.; Barbarella, G. Self-Complementary Nucleoside-Thiophene Hybrid Systems: Synthesis and Supramolecular Organization. *Macromol. Rapid Commun.* **2010**, *31*, 351−355.

(22) Tang, Y.; He, F.; Yu, M.; Feng, F.; An, L.; Sun, H.; Wang, S.; Li, Y.; Zhu, D. A Reversible and Highly Selective Fluorescent Sensor for Mercury(II) Using Poly (Thiophene)S That Contain Thymine Moieties. *Macromol. Rapid Commun.* **2006**, *27*, 389−392.

(23) Humphrey, W.; Dalke, A.; Schulten, K. VMD: Visual Molecular Dynamics. *J. Mol. Graphics* **1996**, *14*, 33−38.

(24) Van Gunsteren, W. F. *Biomolecular Simulation: The GROMOS96 Manual and User Guide*, 1st ed.; Verlag der Fachvereine Hochschulverlag AG an der ETH Zurich: Zurich, Switzerland, 1996.

(25) Marrink, S. J.; Lindahl, E.; Edholm, O.; Mark, A. E. Simulation of the Spontaneous Aggregation of Phospholipids into Bilayers. *J. Am. Chem. Soc.* **2001**, *123*, 8638−8639.

(26) Hess, B.; Bekker, H.; Berendsen, H. J. C.; Fraaije, J. LINCS: A Linear Constraint Solver for Molecular Simulations. *J. Comput. Chem.* **1997**, *18*, 1463−1472.

(27) Berendsen, H. J. C.; Postma, J. P. M.; Vangunsteren, W. F.; Dinola, A.; Haak, J. R. Molecular Dynamics with Coupling to an External Bath. *J. Chem. Phys.* **1984**, *81*, 3684−3690.

(28) Graves, A.; Shivakumar, D.; Boyce, S.; Jacobson, M.; Case, D.; Shoichet, B. Rescoring Docking Hit Lists for Model Cavity Sites: Predictions and Experimental Testing. *J. Mol. Biol.* **2008**, *377*, 914−934.

(29) Pettersen, E. F.; Goddard, T. D.; Huang, C. C.; Couch, G. S.; Greenblatt, D. M.; Meng, E. C.; Ferrin, T. E. UCSF Chimera - a Visualization System for Exploratory Research and Analysis. *J. Comput. Chem.* **2004**, *25*, 1605−1612.

(30) Chirakul, P.; Sigurdsson, S. T. Stereospecific Syntheses of 3′-Deuterated Pyrimidine Nucleosides and Their Site-Specific Incorporation into DNA. *Org. Lett.* **2003**, *5*, 917−919.
(31) Chayer, M.; Faid, K.; Leclerc, M. Highly Conducting Water-Soluble Polythiophene Derivatives. *Chem. Mater.* **1997**, *9*, 2902−2905.
(32) Van Der Spoel, D.; Lindahl, E.; Hess, B.; Groenhof, G.; Mark, A. E.; Berendsen, H. J. C. GROMACS: Fast, Flexible, and Free. *J. Comput. Chem.* **2005**, *26*, 1701−1718.
(33) Berendsen, H. J. C.; Vanderspoel, D.; Vandrunen, R. GROMACS: A Message-passing Parallel Molecular Dynamics Implementation. *Comput. Phys. Commun.* **1995**, *91*, 43−56.